Supporting Information

Cuboidal tethered cyclodextrin frameworks tailored for hemostasis and injured vessel targeting

Yaping He[a, b], Jian Xu[a, b], Xian Sun[a, b], Xiaohong Ren[a], Abi Maharjan[a, b], Peter York[c], Yong Su[d*], Haiyan Li[a, b*], Jiwen Zhang[a, b*]

[a] Center for Drug Delivery Systems, Shanghai Institute of Materia Medica, Chinese Academy of Sciences, 501 Haike Road, Shanghai 201203, China

[b] University of Chinese Academy of Sciences, Beijing 100049, China

[c] Institute of Pharmaceutical Innovation, University of Bradford, Bradford, West Yorkshire BD7 1DP, United Kingdom

[d] Shanghai Fudan-zhangjiang Bio-Pharmaceutical Co., Ltd., Shanghai 201210, China

*E-mail: jwzhang@simm.ac.cn; ysu@fd-zj.com; lihaiyan821005@163.com

Material Characterization

The morphology and size of the samples were characterized by a SEM (JSM-6360LV, JEOL, Akishima, Tokyo, Japan). The specimens were immobilized on a metal stub with double-sided adhesive tape, coated with gold and then observed under definite magnification. The particle size distribution and zeta potential were also measured by the DLS method with a Zetasizer Nano ZS90 instrument (Malvern Panalytical, Malvern, UK). FTIR spectra of samples were obtained using an FTIR spectrometer (Thermo Fisher Nicolet IS5, Thermo Fisher Scientific, Waltham, Massachusetts, USA). Briefly, the powdered sample and KBr crystals were mixed well at a ratio of 1: 10, followed by compression to form a disk. A total of 128 scans were carried out over the wavenumber range of 400-4000 cm^{-1} at a resolution of 4 cm^{-1}. Thermogravimetric analysis (TGA) was carried out using a Pyris 1 thermal analysis system (PerkinElmer, Waltham, Massachusetts, USA) with a temperature ramp from 30 °C to 400 °C at a heating rate of 10 °C per minute under an atmosphere of nitrogen and a final temperature of 400 °C, which was held for 3 min. ^{1}H NMR spectra were recorded at ambient temperature on a Bruker Advance 500 spectrometer (Bruker, Karlsruhe, Baden-Wuerttemberg, Germany), with a working frequency of 400 MHz for ^{1}H nuclei. Stability tests were performed by suspending nanoparticles in water, PBS (pH = 7.4), saline solution and rat serum at 37 °C for seven days, and the release of organic linkers (γ-CDs) at different time points (0, 15 min, 30 min, 1 h, 2 h, 4 h, 8 h, 12 h, 24 h, 3 d, 5 d and 7 d) was quantified by high performance liquid chromatography (HPLC, Figure S1).

Size distribution and Zeta potential analysis

Table S1 The hydrodynamic size distribution and zeta potential of CL-MOF, GS5-MOF, CD-NS and GS5-NS nanoparticles with a concentration of 0.5 mg/mL and the pH was adjusted to 7. All kinds of nanoparticles possess a mean diameter about 200 nm with a very narrow size distribution and a polydispersity index (PDI) less than 0.3.

Samples	DLS Size (nm)	PDI	Zeta potential (mV)	Solvent
CL-MOF	201.8±8.2	0.070	-23.51±0.75	Water
GS5-MOF	199.4±8.9	0.206	-27.20±0.30	Water
CD-NS	203.1±11.7	0.293	-24.90±0.46	Water
GS5-NS	189.4±7.6	0.288	-26.24±0.08	Water

HPLC quantification of γ-CD for stability test

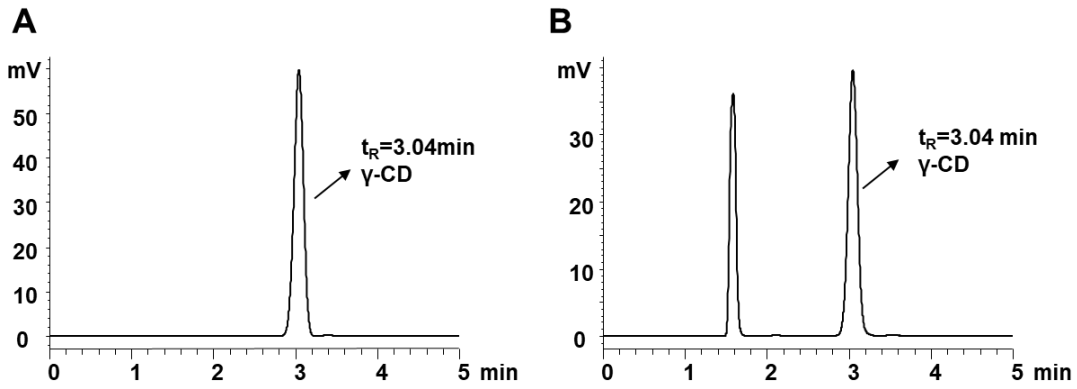

Figure S1 Representative chromatogram of γ-CD reference (A) and γ-CD of the samples (B). The HPLC quantitation of γ-CD was carried out with evaporative light scattering detector (ELSD). The ELSD conditions were set up with the temperature of 70 °C and the filter of 5 s. And the mobile phase was methanol-water (10:90, v/v) with the flow rate of 1 mL·min^{-1}. The experiment was performed with the column temperature of 30 °C and the injection volume of 20 μL.

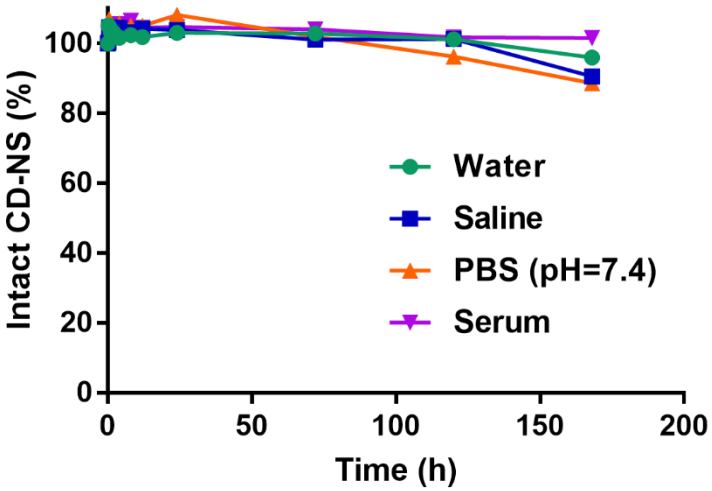

Figure S2 The stability evaluation of CD-NS nanoparticles in water, saline, PBS (pH = 7.4) and serum. CD-NS nanoparticles show good physical stability in above media, with less than 10% free γ-CDs released within seven days.

Cell viability assay

Cell viability was evaluated with MCF-7, HeLa and J774A.1 cells using the Cell Counting Kit-8 (CCK-8) assay, the cells were supplied by Shanghai Cell Bank, Chinese Academy of Sciences (Shanghai, China). Cells were grown in Dulbecco's modified Eagle's medium (DMEM, with phenol red and L-glutamine) supplemented with 10% (v/v) fetal bovine serum (Gibco, Thermo Fisher Scientific, Waltham, Massachusetts, USA), penicillin (100 $IU \cdot mL^{-1}$) and streptomycin (100 $\mu g \cdot mL^{-1}$). Cells were seeded onto 96-well plates at a density of 5000 $cells \cdot well^{-1}$ and maintained in a humidified incubator with 95% air and 5% CO_2 at 37 °C. After incubation overnight, a series of nanoparticle solutions (100 μL; 20, 50, 100, 200, 500 and 1000 $\mu g \cdot mL^{-1}$), were added to the medium and incubated for 12 h. Then, CCK-8 solution (20 μL) was added to each well and incubated for 2 h, and the absorbance was measured at 450 nm (reference wavelength of 630 nm) using a microplate reader (Multiskan GO, Thermo Fisher Scientific, Waltham, Massachusetts, USA). Six replicate wells were used for control and test concentration per microplate. Nontreated cells were used as a blank control, and the cell viability (%) was calculated by following formula (S1). The results are expressed as the mean ± standard deviation.

$$\text{Cell viability (\%)} = \frac{A_{sample} - A_{blank}}{A_{control} - A_{blank}} \times 100 \qquad \text{(S1)}$$

The cytotoxicity of spherical CD-NS nanoparticles in different cell lines

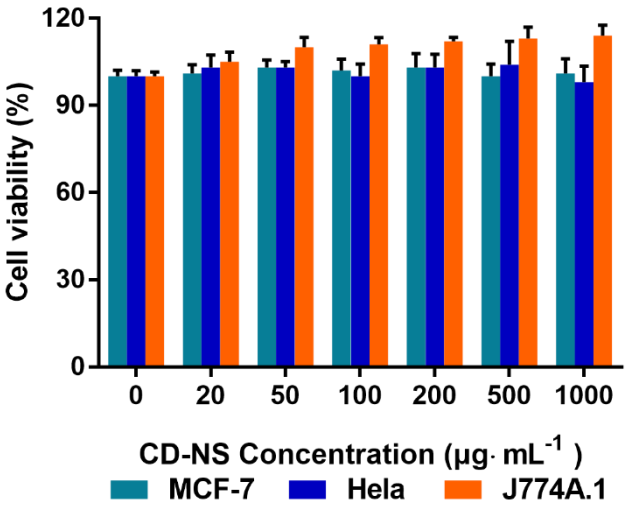

Figure S3 The cellular toxicity of CD-NS nanoparticles were evaluated by MTT assay. CD-NS nanoparticles show a biofriendly nature and no cytotoxic effects were observed in MCF-7, Hela and J774A.1 cell lines up to the concentration of 1000 μg·mL^{-1}.

Hemolysis assay

The hemolysis of GS5-MOF nanoparticles was examined by spectrophotometry. The SD rat red blood cells were obtained by centrifugation of freshly collected citrated blood at 2500 rpm for 10 min to remove the serum and further washed three times with normal saline solution. And the red cells were diluted to 2% (v/v) with normal saline. CL-MOF, GS5-NS and GS5-MOF nanoparticles were dispersed into saline solution at concentrations ranging from 100 to 1000 μg·mL^{-1}. Saline solution and ultrapure water were used as negative and positive controls, respectively. Then, 1.5 mL of the diluted rat red blood cell suspension was mixed with 1.5 mL above samples. The mixtures were incubated at 37 ℃ for 3 h and centrifuged for 15 min at 1500 rpm, the absorbances of the supernatant at 541 nm were recorded by the spectrophotometer (HITACHI UH5300, Tokyo, Japan). All hemolysis experiments were performed in triplicates. The hemolysis ratio was calculated as the equation (S2):

$$\text{Hemolysis ratio}\ (\%) = \frac{\mathrm{A_{sample}} - \mathrm{A_{negative\ control}}}{\mathrm{A_{positive\ control}} - \mathrm{A_{negative\ control}}} \times 100 \qquad (S2)$$

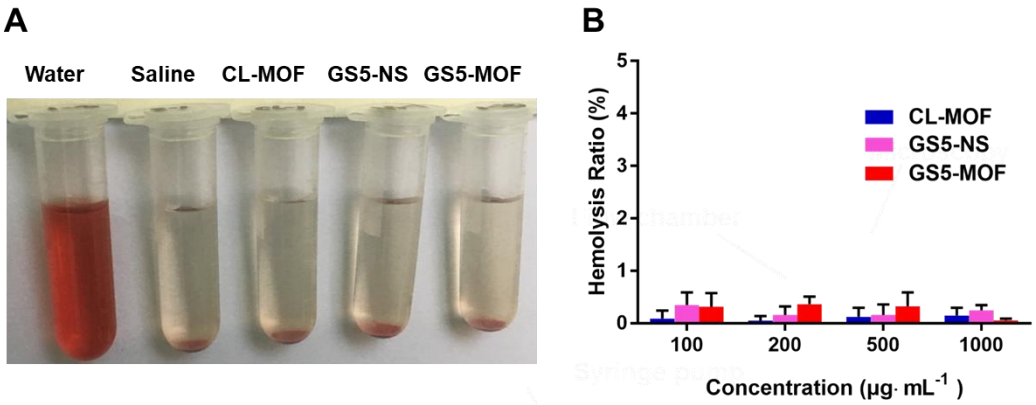

Figure S4 Hemolysis test of CL-MOF, GS5-NS and GS5-MOF nanoparticles. The hemolysis ratios are less than 1% as the concentrations increased to 1000 μg·mL^{-1}. It is generally considered safe for injection when hemolysis ratio is less than 5%, indicating good blood compatibility of GS5-MOF nanoparticles. (A) The experimental image of hemolysis assay at the concentration of 1000 μg·mL^{-1}. (B) Hemolysis ratio of CL-MOF, GS5-NS and GS5-MOF nanoparticles. The results are expressed as the mean ± SD (n = 3).

^{1}H-NMR spectrum analysis

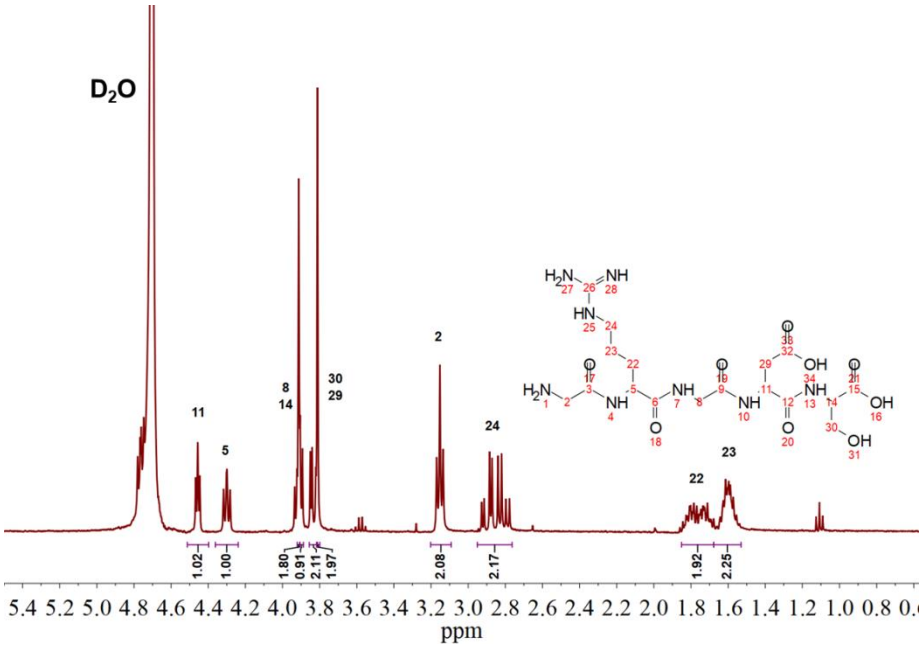

Figure S5 ^{1}H-NMR spectrum of GRGDS in D_2O, the characteristic peaks for GRGDS protons (δ = 2.7~2.9, 3.2, 3.9, 4.3 ppm) were readily observable and assigned.

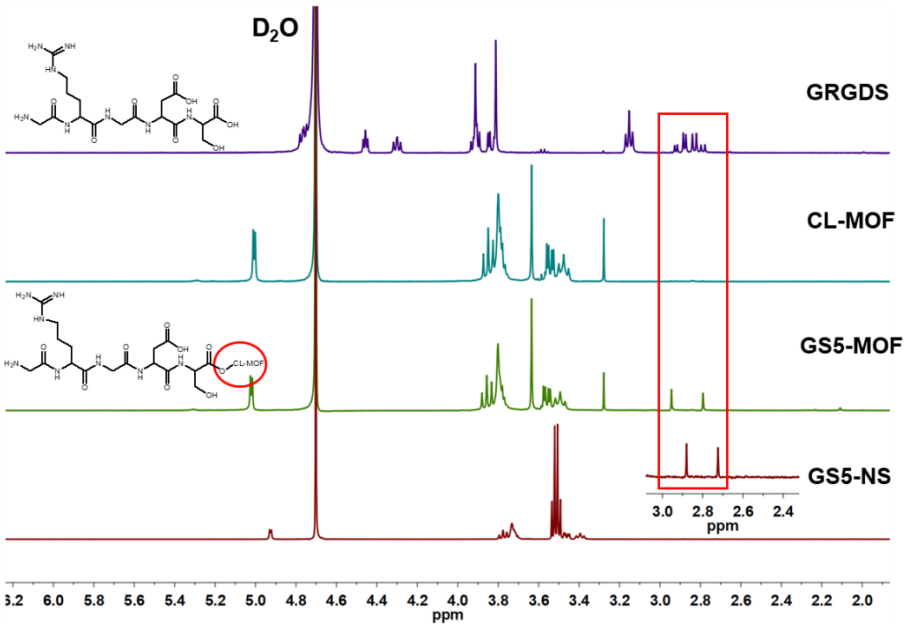

Figure S6 ^{1}H-NMR spectra of CL-MOF, GS5-MOF and GS5-NS nanoparticles in D_2O with NaOD, GRGDS proton (δ = 2.7~2.9 ppm) related peaks confirmed the successful modification of GRGDS on the surface of two types of the nanoparticles.

HPLC quantification of GRGDS on GS5-MOF and GS5-NS nanoparticles

Table S2 The HPLC methodology validation for the quantification of GRGDS. The HPLC analysis was carried out with Agilent 1260. A Dikma C18 column (5 μm, 4.6 mm×150 nm) was used with flow rate of 1.0 $mL \cdot min^{-1}$ at a wavelength of 220 nm and the column temperature of 25 °C. The mobile phase was composed of 3% acetonitrile in 0.1% phosphoric acid aqueous solution.

Items	40 $\mu g \cdot mL^{-1}$	160 $\mu g \cdot mL^{-1}$	800 $\mu g \cdot mL^{-1}$
Precision (RSD %)	1.19	0.56	0.53
Stability (%)	100.15	100.2	100.06
Recovery rate (%)	107.73	100.43	100.05
Limit of quantitation ($\mu g \cdot mL^{-1}$)	8		
Limit of detection ($\mu g \cdot mL^{-1}$)	2.5		
Standard curve	$A = 1.1096\ C + 2.6377$, $R^2 = 1$		

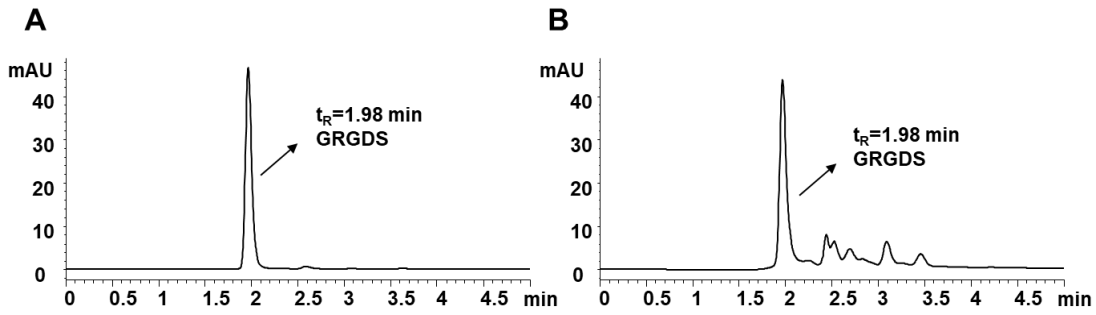

Figure S7 Representative chromatogram graph of GRGDS (A) and GS5-MOFs (B). By using the above HPLC method, the content of GRGDS in GS5-MOF and GS5-NS nanoparticles was measured as 0.5 wt%.

TGA analysis

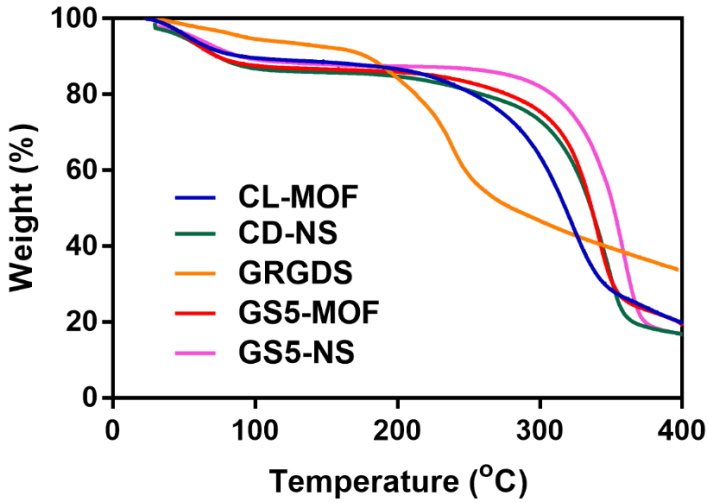

Figure S8 TGA of CL-MOF, CD-NS, GS5-NS and GS5-MOF nanoparticles. In the range of 250 to 350 ℃, GRGDS modified GS5-MOF and GS5-NS nanoparticles showed less weight loss than that for the unmodified CL-MOF and CD-NS nanoparticles, respectively.

In vitro adhesion and aggregation of GS5-MOFs with activated platelets under shear stresses

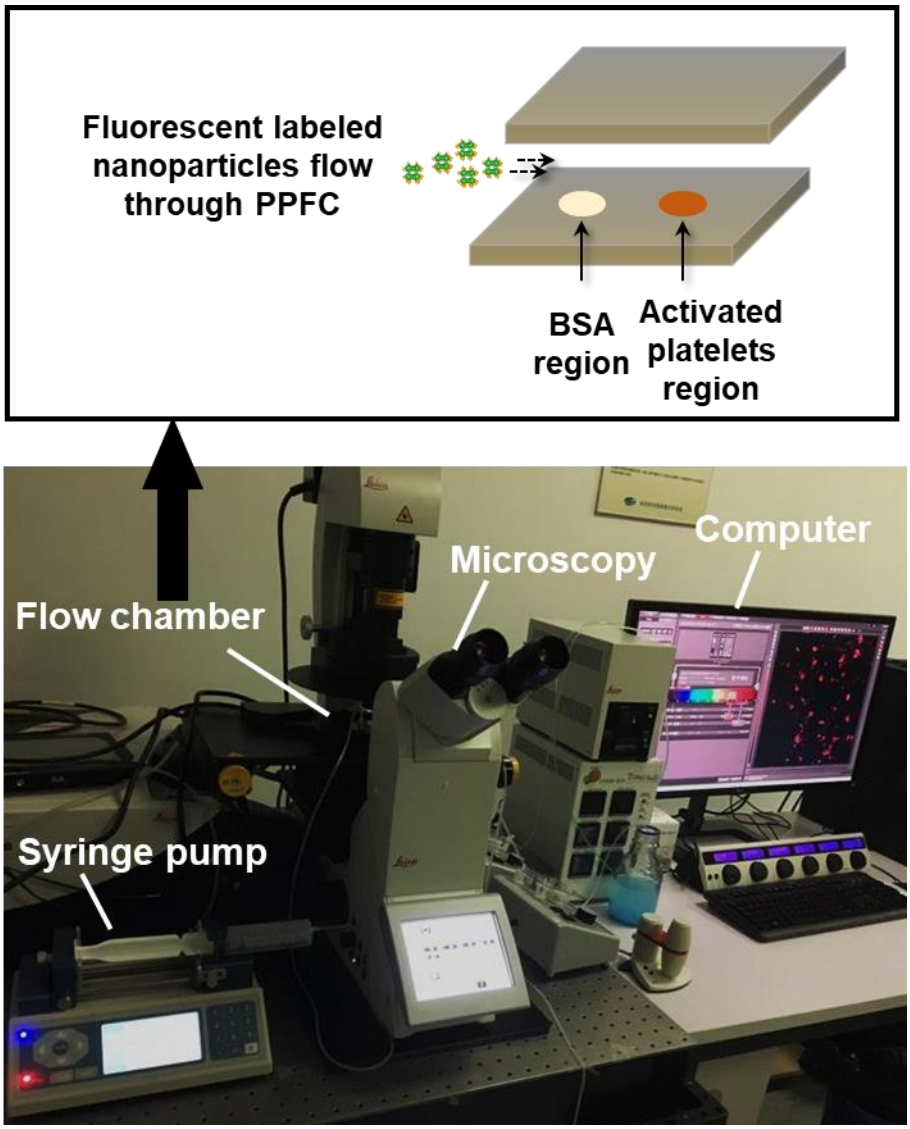

Figure S9 Experimental setup for PPFC in vitro aggregation studies.

AFM measurement of adhesion force between nanoparticles and activated platelets

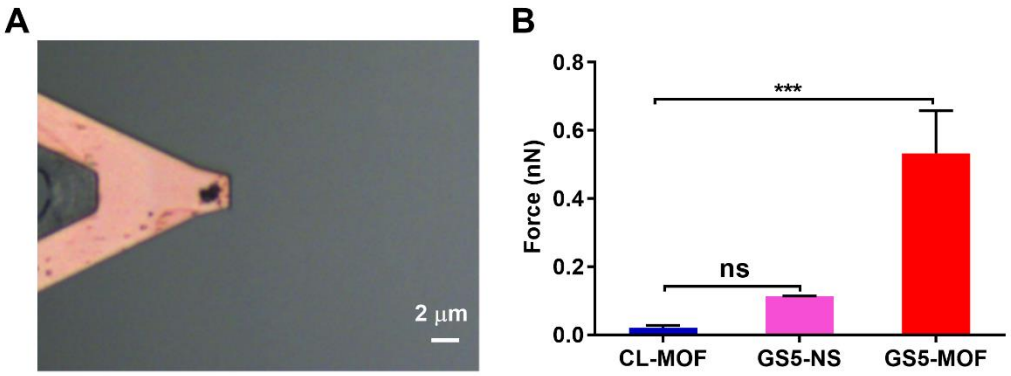

Figure S10 Microscopy image of the AFM cantilever immobilized with GS5-MOF nanoparticles (A) and the quantitative adhesion force (B) for the interaction of CL-MOF, GS5-NS and GS5-MOF nanoparticles with activated platelets. Data are expressed as the mean ± SD (n =10). ***p < 0.001, the abbreviation ns denotes no statistical difference between CL-MOF and GS5-NS groups.

The aggregates formed of activated platelets with GS5-MOFs

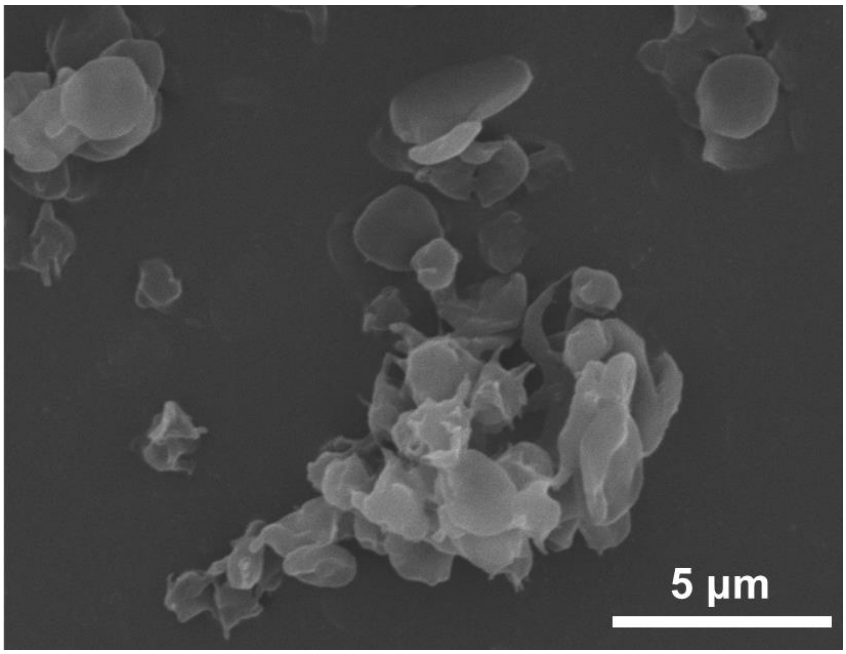

Figure S11 A typical SEM image of activated platelets aggregated with GS5-MOF nanoparticles.

Table S3 Size changes by the formation of aggregates with activated platelets.

Samples	DLS Size (nm)	PDI
GS5-MOF	199.4±8.9	0.206
Quiescent platelets	2139±479	0.285
Aggregated platelets with GS5-MOF	4726±881	0.291

The influences of GS5-MOFs on hemostasis balance in SD rats

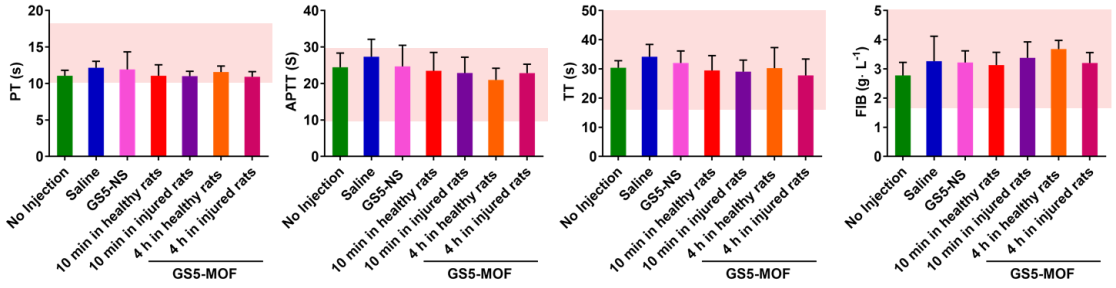

Figure S12 Typical coagulation parameters of rats after injection of GS5-MOF nanoparticles at 28 mg·kg^{-1} (n = 6). PT, prothrombin time; APTT, activated partial thromboplatin time; TT, thrombin time; FIB, fibrinogen content. The pink windows indicate the normal levels of different parameters. The coagulation indicators including PT, APTT, TT and FIB were all in the normal range, indicating that the GS5-MOFs had no influences on coagulation function and could not trigger unwanted thrombosis in SD rats.

Targeting efficiency in a mouse tail transection model evaluated by microCT imaging

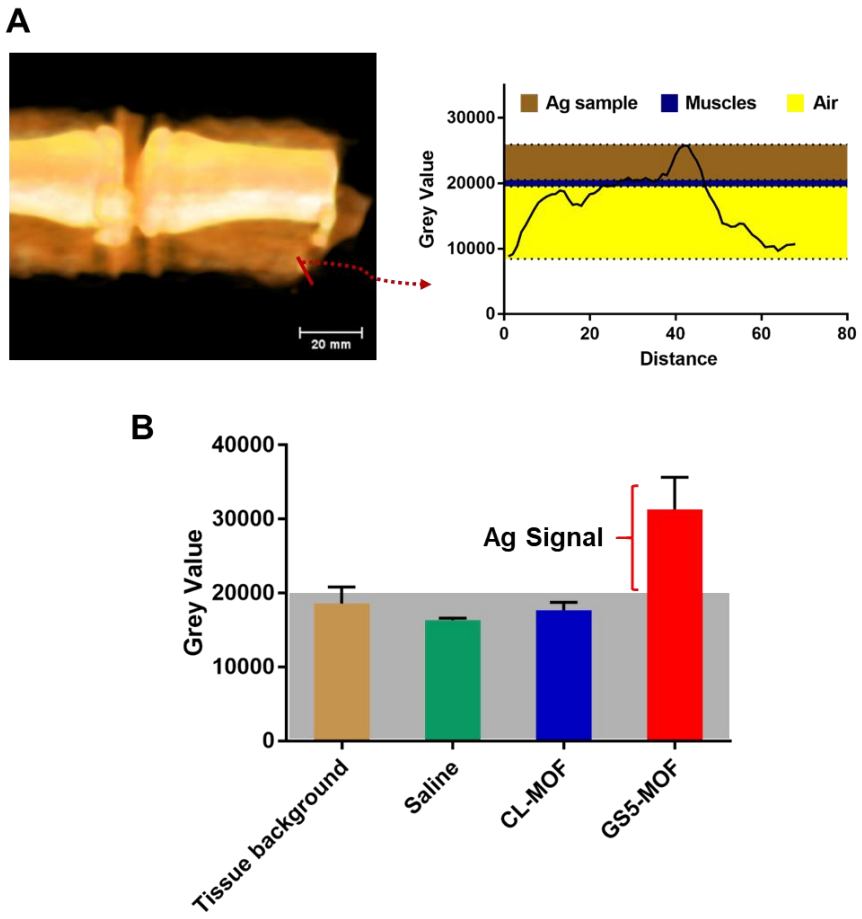

Figure S13 The targeting capacity study of GS5-MOF nanoparticles in the transected mouse tail by microCT technique. (A) The gray value of peripheral tissue background was lower than 20000, while the gray value for silver signal concentrated in the mouse tail clot was between 20000 and 30000. (B) Ag@GS5-MOF nanoparticles can specifically target and accumulate at the injured vessels.

174 **Quantitation of silver content by ICP-MS**

Table S4 The silver content of transected mouse tail was quantified via ICP-MS. The GS5-MOF nanoparticles treated tail displayed 7-fold increased silver signal compared to saline control.

Samples	Silver content ($mg \cdot kg^{-1}$)
Saline treated tail	0.202
CL-MOF treated tail	0.44
GS5-MOF treated tail	1.34

175

176

References

S1. Smaldone RA, Forgan RS, Furukawa H, Gassensmith JJ, Slawin AM, Yaghi OM, et al. Metal-organic frameworks from edible natural products. Angew Chem Int Ed Engl. 2010; 49: 8630-4.

S2. Rojas MJ, Castral TC, Giordano RL, Tardioli PW. Development and validation of a simple high performance liquid chromatography-evaporative light scattering detector method for direct quantification of native cyclodextrins in a cyclization medium. J Chromatogr A. 2015; 1410: 140-6.

S3. Horcajada P, Chalati T, Serre C, Gillet B, Sebrie C, Baati T, et al. Porous metal-organic-framework nanoscale carriers as a potential platform for drug delivery and imaging. Nat Mater. 2010; 9: 172-8.

S4. Li J, Guo Y. Basic evaluation of typical nanoporous silica nanoparticles in being drug carrier: Structure, wettability and hemolysis. Mater Sci Eng C Mater Biol Appl. 2017; 73: 670-3.

S5. Barendrecht AD, Verhoef JJF, Pignatelli S, Pasterkamp G, Heijnen HFG, Maas C. Live-cell imaging of platelet degranulation and secretion under flow. J Vis Exp. 2017; 125: doi: 10.3791/55658.

S6. Feghhi S, Sniadecki NJ. Mechanobiology of platelets: techniques to study the role of fluid flow and platelet retraction forces at the micro- and nano-scale. Int J Mol Sci. 2011; 12: 9009-30.

S7. Cui Y, Yang J, Zhou Q, Liang P, Wang Y, Gao X, et al. Renal clearable Ag nanodots for in vivo computer tomography imaging and photothermal therapy. ACS Appl Mater Interfaces. 2017; 9: 5900-6.